


A multi-proxy investigation of late-Holocene temperature change and climate-driven fluctuations in sediment sourcing: Simpson Lagoon, Alaska

The Holocene
1–14
© The Author(s) 2018
Reprints and permissions:
sagepub.co.uk/journalsPermissions.nav
DOI: 10.1177/0959683617752845
journals.sagepub.com/home/hol


Andrea JM Hanna,¹ Timothy M Shanahan,² Mead A Allison,^{3,4} 
Thomas S Bianchi⁵ and Kathryn M Schreiner⁶

Abstract

The significant and ongoing environmental changes in Arctic regions demonstrate the need for quantitative, high-resolution records of pre-industrial climate change in this climatically sensitive region; such records are fundamental for understanding recent anthropogenic changes in the context of natural variability. Sediment contained within Arctic coastal environments proximal to large fluvial systems has the ability to record paleoclimate variability on subdecadal to decadal scale resolution, on par with many other terrestrial climate archives (i.e. lake sediments, ice cores). Here, we utilize one such sediment archive from Simpson Lagoon, Alaska, located adjacent to the Colville River Delta to reconstruct temperature variability and fluctuations in sediment sourcing over the past 1700 years. Quantitative reconstructions of summer air temperature are obtained using the branched glycerol dialkyl glycerol tetraether (brGDGT)-derived methylation index of branched tetraethers (MBT)/cyclization ratio of branched tetraether (CBT) paleothermometer and reveal temperature departures correlative with noted climate events (i.e. 'Little Ice Age', 'Medieval Climate Anomaly'). In addition, temporal variability in sediment sourcing to the lagoon, determined using a multi-proxy approach (i.e. granulometry, elemental analysis, clay mineralogy), broadly corresponds with temperature fluctuations, indicating relative increases in fluvial sediment discharge during colder intervals and decreased river discharge/increased coastal erosion during warmer periods. The Simpson Lagoon record presented in this study is the first temperature reconstruction, to our knowledge, developed from coastal marine sediments in the Alaskan Beaufort Sea.

Keywords

Alaska, Arctic, Colville Delta, Estuarine sediments, late Holocene, paleoclimate

Received 3 August 2017; revised manuscript accepted 8 December 2017

Introduction

Arctic regions are highly sensitive to both natural and anthropogenic climate forcings, as evidenced by the recent warming trend over the past century and the significant climate variability observed throughout the late Holocene (e.g. Kaufman et al., 2009; McKay and Kaufman, 2014; Overpeck et al., 1997; Serreze et al., 2000). Instrumental temperature records from North America over the past century indicate that the greatest warming has occurred in the highest latitudes (IPCC, 2013; Miller et al., 2010), leading to significant and pervasive environmental changes including enhanced permafrost degradation (Batir et al., 2017; Lachenbruch and Marshall, 1986), extreme rates of coastal erosion (Jones et al., 2009; Mars and Houseknecht, 2007), increased rates of glacial melt (Berthier et al., 2010; Evison et al., 1996), and decreases in the duration and extent of sea ice and snow cover (Mahoney et al., 2007; Stone and Longenecker, 2001).

Due to the relatively short (~60 years) and spatially limited instrumental records (e.g. temperature, precipitation, river discharge) in the Arctic, paleoenvironmental proxy records are critical for extending our knowledge of climate variability back through time, allowing for recent and future changes in these climate variables to be evaluated against long-term natural variability. Numerous high-resolution paleoclimate records spanning the

past few millennia have been developed throughout the Arctic and reveal annual, decadal, and centennial-scale variations in the climate system (e.g. Kaufman et al., 2009; McKay and Kaufman, 2014 and references therein). In Alaska, reconstructions of late-Holocene climate (i.e. temperature, precipitation) reveal widespread pre-industrial climate perturbations such as the 'Little Ice

¹Institute for Geophysics, Jackson School of Geosciences, University of Texas at Austin, USA

²Department of Geosciences, Jackson School of Geosciences, University of Texas at Austin, USA

³Department of Earth and Environmental Sciences, Tulane University, USA

⁴The Water Institute of the Gulf, USA

⁵Department of Geological Sciences, University of Florida, USA

⁶Department of Chemistry and Biochemistry and Large Lakes Observatory, University of Minnesota Duluth, USA

Corresponding author:

Mead A Allison, Department of Earth and Environmental Sciences, Tulane University, Blessey Hall, New Orleans, LA 70118-5665, USA.
Email: meadallison@tulane.edu

Age' (LIA) and 'Medieval Climate Anomaly' (MCA), albeit with local variability in the timing and magnitude of these anomalies (e.g. Bird et al., 2009; Boldt et al., 2015; Chipman et al., 2012; Clegg and Hu, 2010; Loso, 2009).

The majority of these existing Arctic paleoclimate records are derived from tree-ring and lake-sediment analyses (e.g. McKay and Kaufman, 2014). In the tundra that comprises the Alaskan high Arctic, the paucity of tree ring data makes it necessary to rely on sediment archives from lakes and coastal marine environments for these high-resolution climate records. Whereas lake sediments are the most prevalent paleoclimate archives in the Arctic, they only provide terrestrial climate signals and are often integrated over a relatively limited catchment area. Currently, very few paleoclimate archives have been developed from Arctic coastal sediments, despite the fact that delta-front estuaries adjacent to Arctic rivers often contain high-resolution, continuous sediment archives that have the unique ability to provide information on both terrestrial and marine climate variability (Bianchi and Allison, 2009; Hanna et al., 2014).

In addition to providing a potential archive for paleotemperature reconstruction, coastal marine sediments may also record climate-linked temporal fluctuations in the magnitude and character of terrestrial and marine sediment sources reaching the coastal depositor. In Arctic Alaska, sedimentation in coastal environments is dominated by fluvial sediment input and coastal erosion that either originates locally or is delivered alongshore by coastal currents (Jones et al., 2009; Rachold et al., 2000; Schreiner et al., 2013). Variability in fluvial discharge is primarily a response to net precipitation changes in unglaciated Arctic systems (McClelland et al., 2006; Peterson et al., 2002). Therefore, fluctuations in fluvially derived sediment may illustrate changes in the effective moisture balance, which in turn are likely influenced by temperature and large-scale atmosphere–ocean circulation (Dery et al., 2009; Peterson et al., 2002). The fluvial discharge of many Arctic rivers has significantly increased during the latter half of the 20th century (Dery et al., 2009; McClelland et al., 2006; Peterson et al., 2002), in part due to increased moisture transport to higher latitudes resulting from global warming (McClelland et al., 2004; Stocker and Raible, 2005). Predicted future atmospheric and sea-surface warming is anticipated to accelerate this trend, with an estimated increase in fluvial sediment flux to the Arctic Ocean of ~30% per 2°C atmospheric warming (Gordeev, 2006). However, unlike the Arctic Eurasian rivers, North American river discharge to the Arctic Ocean has displayed an overall decrease in fluvial input over the latter half of the 20th century (McClelland et al., 2006). Therefore, discharge fluctuations of these North American rivers, in particular, need to be further evaluated to clarify their potential responses to anticipated future warming.

In addition, coastal erosion is accelerating throughout the Arctic, with shoreline retreat rates in Arctic Alaska doubling over the past 50 years (Jones et al., 2009; Mars and Houseknecht, 2007). This trend has been attributed to increased sea-surface and air temperature, longer duration of ice-free season, sea-level rise, and increased magnitude and frequency of storms (Jones et al., 2009). Therefore, Arctic estuarine sediments may contain long-term records of temporal changes in the relative magnitude of shoreline-derived sediment input and provide additional insight into the potential driving mechanisms of shoreline retreat in these regions.

This study aims to produce a new ~1700-year paleoclimate archive for the high Arctic utilizing coastal marine sediments from Simpson Lagoon, Alaska, located on the inner Beaufort shelf adjacent to the Colville River mouth. Here, we use a multi-proxy approach, using the methylation index of branched tetraether (MBT)/cyclization ratio of branched tetraether (CBT) paleothermometer (Peterse et al., 2012) to reconstruct summer air temperatures and major elements, grain size, and clay mineralogy

to identify variations in fluvial discharge and coastal erosion, which likely result from climate-driven processes. Finally, we compare the records from Simpson Lagoon with previously published regional reconstructions from other terrestrial archives (i.e. tree ring, lake sediment) to evaluate the potential of Arctic coastal sediment archives for paleoenvironment reconstructions.

Regional setting

Simpson Lagoon is a shallow (<2.5 m water depth) back-barrier estuary located immediately east of the Colville River Delta on the inner shelf of the Alaskan Beaufort Sea (Figure 1). The lagoon is covered annually with shorefast ice for ~8–9 months yr⁻¹ (Reimnitz et al., 1978), resulting in terrigenous inputs to the lagoon that are focused between the months of June through September. Despite this seasonality, modern sediment accumulation is relatively rapid (0.02–0.46 cm yr⁻¹; Hanna et al., 2014), likely due to the proximity of the Colville River and a mainland permafrosted tundra shoreline that is rapidly retreating (Jorgenson et al., 2006; Mars and Houseknecht, 2007). In addition, the high sedimentation rates may also be a function of the sediment-trapping potential afforded by restricted (estuarine) circulation generated by the Jones Island barrier chain. The lagoonal sediment record is relatively continuous over the past ~3500 years and is stratigraphically undisturbed by the sea ice processes that disrupt many Arctic marine sediment archives due to the presence of landfast ice and the sheltering effects afforded by the barrier islands (Hanna et al., 2014).

The largest potential source of sediment to Simpson Lagoon is the Colville River (Schreiner et al., 2013). The Colville catchment (53,000 km³) extends from the north slope of the central Brooks Range to the Alaskan Beaufort Sea and encompasses portions of Alaska's Arctic Foothills and Arctic Coastal Plain. Low mean annual temperatures on the North Slope of Alaska (–11°C; NOAA National Climate Data Center) lead to continuous permafrost in the organic-rich soils within the catchment (Eisner et al., 2005; Lachenbruch and Marshall, 1969; Osterkamp and Payne, 1981). The hydrology of the Colville River is dominated by the late spring/early summer snowmelt, with observed peak water discharges in excess of 6000 m³ s⁻¹ (Arnborg et al., 1967; Walker and Hudson, 2003). This freshet also transports the majority of the annual suspended sediment flux (6 × 10⁶ ton yr⁻¹) so that 62% of the fluvial sediment input to the delta and coastal zone is delivered during a 2-week period (Arnborg et al., 1967; Walker and Hudson, 2003). Despite relatively low mean annual precipitation in the Colville catchment (48.4 cm yr⁻¹; McClelland et al., 2014), significant fluvial discharge resulting from rainfall events is also possible, albeit infrequent, during the summer months when precipitation is at a maximum (Mock et al., 1998; Ray and Aldrich, 1996). Measurements of the Colville River water discharge and sediment flux are limited (Arnborg et al., 1967; McClelland et al., 2014; Trefry et al., 2009), therefore the effects of the 20th century warming trend on fluvial discharge are largely unknown.

In addition to fluvial input, coastal erosion is a significant source of sediment and organic material to Simpson Lagoon (Schreiner et al., 2013, 2014; Zhang et al., 2015). The mainland coastline of Simpson Lagoon is bordered by a narrow sand beach backed by peat-rich tundra bluffs approximately 1 m in height (Jorgenson and Brown, 2005). Erosion of this organic-rich shoreline tundra has been found to contribute up to seven times as much sediment to the Alaskan Beaufort shelf as fluvial input (Rachold et al., 2000). In Simpson Lagoon alone, erosion of the tundra shoreline occurred at an average rate of 1.2 m yr⁻¹ between 1970 and 1980, amounting to an annual sediment contribution of 685 MT km⁻¹ (approximately 75,000 MT yr⁻¹) (Jorgenson and Brown, 2005).

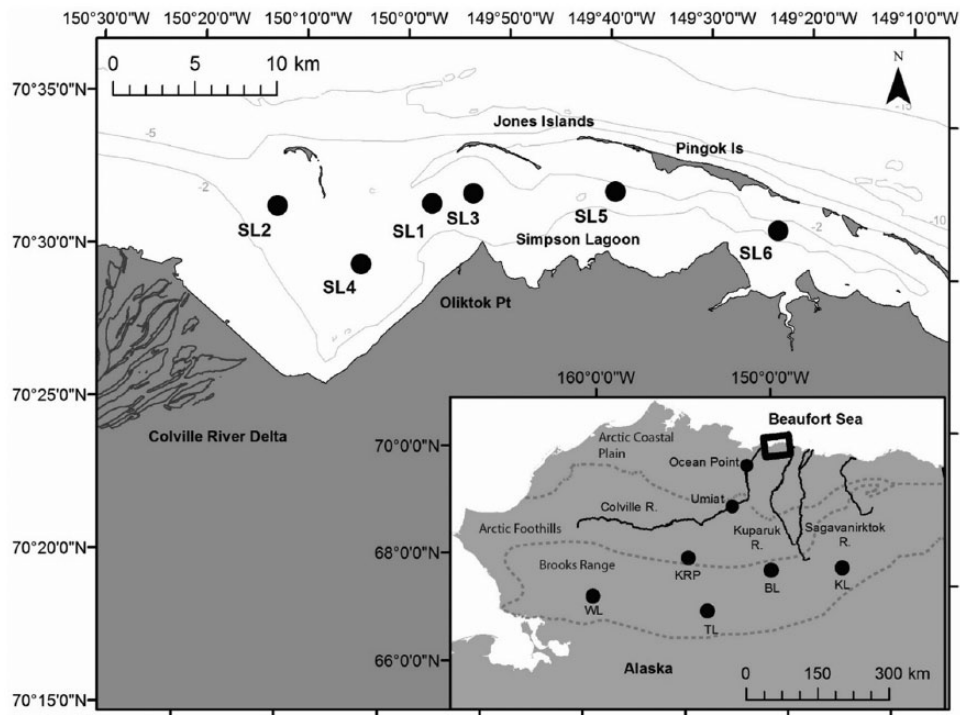


Figure 1. Map of Simpson Lagoon, AK study area with locations of sediment cores collected during the August 2010 field study. Inset includes locations of North Slope Alaska paleoclimate records mentioned in text (WL: Wolverine Lake; KRP: Kurupa Lake; TL: Takahula Lake; BL: Blue Lake; KL: Keche Lake). North Slope provinces (i.e. Arctic Coastal Plain, Arctic Foothills, Brooks Range) are delineated by dashed lines.

Materials and methods

Field techniques and sampling

Sediment cores between 76 and 264 cm in length were collected from Simpson Lagoon using a Rossfelder P-3 submersible vibracorer aboard the R/V *Annika Marie* in August 2010 (Figure 1). Cores were split lengthwise onboard, with one half sectioned into 2-cm intervals and the other core-half x-rayed on site and shipped to the University of Texas laboratory for whole core analyses (e.g. XRF core logger) before being sub-sampled at 1-cm intervals. For the purpose of this study, we will focus on core SL4, as radiocarbon analysis has revealed this core to contain a continuous, ~1700-year record with a relatively high (1.5 mm yr^{-1}) and constant accumulation rate (Hanna et al., 2014). In addition, this core has been documented to receive organic material from both coastal erosion and fluvial input and, therefore, is likely a viable location to assess temporal variability in sediment sourcing (Schreiner et al., 2013).

A subsequent field study was conducted in August, 2012 along the Colville River between Umiat, AK ($69^{\circ}22'01''\text{N}$, $152^{\circ}08'39''\text{W}$) and Ocean Point, AK ($70^{\circ}3'55''\text{N}$, $151^{\circ}23'12''\text{W}$) (Figure 1). A total of 26 surface grab samples (upper 5–10 cm) and nine short push cores (<65 cm) were collected from various environments (e.g. Colville River channel, fluvial braid bars, floodplain lakes, catchment tundra, and Cretaceous and Pliocene/Pleistocene outcrops). These samples supplement surface sediment samples collected in 2010 from shoreline sediment near Oliktok Point, Pingok Island, and the Sagavanirktok Delta (~100 km east of Simpson Lagoon) and are utilized in characterization of potential sediment sources to Simpson Lagoon. All samples were freeze-dried and lightly ground before proceeding with sedimentological and geochemical analyses.

Geochronology

A detailed description of the geochronology conducted on Simpson Lagoon core SL4 is presented in Hanna et al. (2014), but a brief summary is given here. A multi-radiotracer approach

consisting of ^{137}Cs , $^{239,240}\text{Pu}$, and ^{14}C was utilized to determine the geochronology of Simpson Lagoon core SL4. Modern (~50 years) sediment accumulation rates were calculated using the bomb-tracers ^{137}Cs and $^{239,240}\text{Pu}$ measured via gamma spectrometry and inductively coupled plasma mass spectrometry (ICP-MS), respectively. Activity profiles of these radiotracers exhibit maximum activity peaks corresponding with the 1963/1964 maximum global fallout from nuclear weapons testing, the depth of which can be used as a chronostratigraphic marker. Errors associated with modern accumulation rates are calculated to be $\pm 0.04 \text{ cm yr}^{-1}$ and are a function of the sample resolution.

In addition, six radiocarbon ages of mixed benthic foraminifera (*Elphidium* sp. and *Buccella frigida*) were obtained for core SL4 by accelerator mass spectrometry (AMS) performed at the NOSAMS facility at the Woods Hole Oceanographic Institution. The age model and associated uncertainty determined from the ^{137}Cs and radiocarbon dates were generated using a Bayesian technique for calibration and age modeling utilizing the R software package BACON (Blaauw and Christen, 2011) in conjunction with the Marine13 radiocarbon calibration curve (Reimer et al., 2013). The results of the SL4 age model are shown in Figure 2.

Glycerol dialkyl glycerol tetraether analysis

Branched glycerol dialkyl glycerol tetraethers (brGDGTs) are microbial membrane lipids primarily found in soil organic material and commonly transported to coastal marine sediments via rivers (Hopmans et al., 2004; Rueda et al., 2009; Weijers et al., 2007a). Nine individual brGDGTs, containing four to six methyl substituents and zero to two cyclopentyl moieties on linear C_{28} alkyl chains, were originally described by Sinninghe Damste et al. (2000) with the degree of methylation and cyclization influenced primarily by temperature and soil pH (Peterse et al., 2012; Weijers et al., 2007b). An additional set of six brGDGT isomers containing methyl groups at the sixth position has been recently identified by De Jonge et al. (2013, 2014a), though these isomers were not resolved in the extraction and analysis methods described here. The structures of all 15 brGDGT compounds are illustrated in Figure 3.

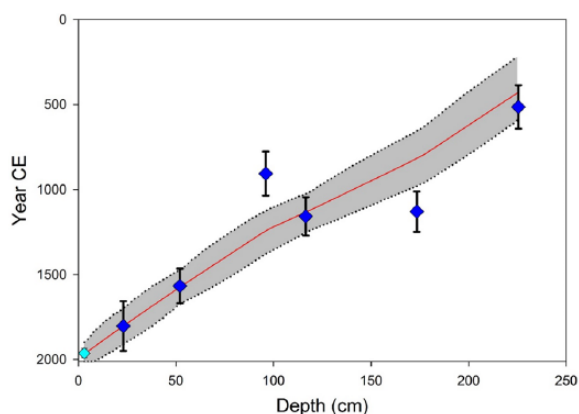


Figure 2. Age–depth model for Simpson Lagoon core SL4 with ^{137}Cs chronostratigraphic horizon (light blue) and calibrated radiocarbon dates (dark blue). Red line indicates median calculated value and gray stippled lines outline the 95% confidence interval.

To expand upon previous brGDGT analysis spanning the past 75 years in Simpson Lagoon (core SL2; Hanna et al., 2016), measurements of brGDGTs were obtained every 3 cm (~20-year resolution) in Simpson Lagoon core SL4, and the extraction and analysis method is described in detail there. Briefly, the total lipid fraction was extracted in a 9:1 dichloromethane (DCM):methanol solution via microwave extraction (MARS 5 Xpress, CEM Corporation). Activated copper powder was added to the samples to remove elemental sulfur before filtering the samples and rinsing with hexane (2 \times) and DCM (3 \times). The total lipid extract was fractionated over an aminopropyl column into apolar, ketone, polar, and fatty acid fractions using eluents of hexane, 4:1 hexane:DCM, 9:1 DCM:acetone, and 2% formic acid in DCM, respectively. All fractions were dried using N_2 and re-dissolved in a solution of 1% isopropanol in hexane.

The polar fraction was analyzed for brGDGTs via high-performance liquid chromatography–atmospheric pressure chemical ionization mass spectrometry (HPLC-APCI-MS) on an Agilent 1200 HPLC instrument fitted with a Prevail Cyano column (150 mm \times 2.1 mm i.d., 3 μm). Separation was achieved using an initial solvent composition of 1% isopropanol in hexane maintained at 0.2 mL min^{-1} for 5 min, followed by a ramped increase to 1.5% isopropanol in hexane over a period of 28.1 min (Schouten et al., 2007). The mass spectrometer was operated in single ion monitoring (SIM) mode using m/z 1022, 1020, 1018, 1036, 1034, 1032, 1050, 1048, 1046 for the branched GDGTs Ia, Ib, Ic, IIa, IIb, IIc, IIIa, IIIb, IIIc, respectively. Relative abundance of individual brGDGTs was determined by integrating the peak areas of the protonated molecule using Agilent Chemstation software. All raw brGDGT results are presented in Supplementary Table 1 (available online).

BrGDGT indices quantifying the degree of CBT and the extent of MBT' were calculated using Eqs 1 and 2 (Peterse et al., 2012; Weijers et al., 2007b), where the roman numerals correspond to the brGDGT structures in Figure 3:

$$\text{CBT} = -\log \left[\frac{(\text{Ib} + \text{IIb})}{(\text{Ia} + \text{IIa})} \right] \quad (1)$$

$$\text{MBT}' = \frac{\text{Ia} + \text{Ib} + \text{Ic}}{\text{Ia} + \text{Ib} + \text{Ic} + \text{IIa} + \text{IIb} + \text{IIc} + \text{IIIa}} \quad (2)$$

$$\text{MAT} = 0.81 - 5.67 \cdot \text{CBT} + 31.0 \cdot \text{MBT}' \quad (3)$$

The reconstructed continental mean air temperature (MAT) of each sample was calculated using Eq. 3, which is derived from the

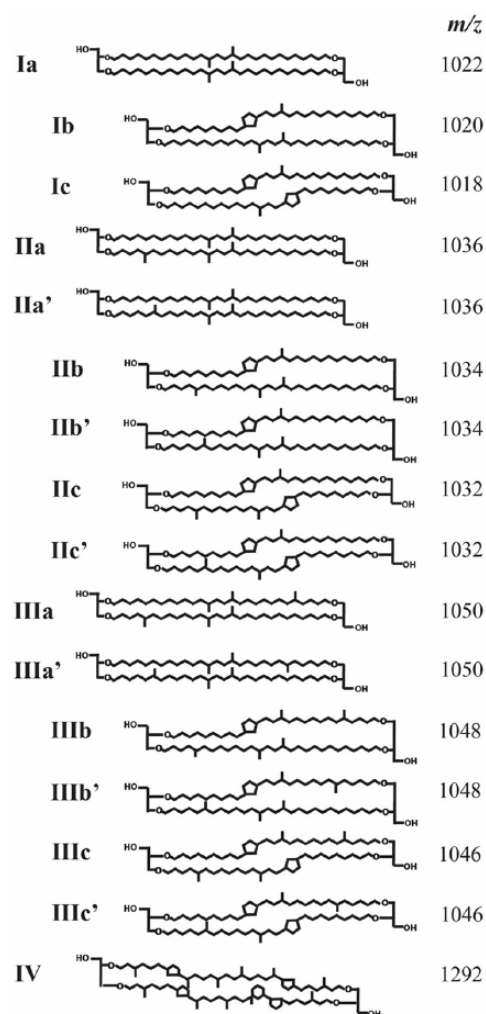


Figure 3. Structures of branched GDGTs, including the recently identified 6-methyl brGDGT isomers utilized in the MBT'/CBT paleothermometer, and crenarchaeol (IV).

global soil calibration of Peterse et al. (2012). The residual standard mean error for the calibration data set is 5.7 $^{\circ}\text{C}$. A bootstrapping method (Efron, 1979) with 1000 resamples for the calibration dataset was applied to the Simpson Lagoon reconstructions to determine errors in the reconstructed MATs following the methods of Loomis et al. (2012).

x-Ray fluorescence analysis

x-Ray fluorescence (XRF) analysis was performed on the split core from SL4 at a 1-cm measurement interval prior to subsampling. Measurements were made using a third-generation Avaatech XRF core scanner equipped with a Rh-anode x-ray tube at the Ocean Drilling and Sustainable Earth Science Laboratory in the IODP research facility, College Station, TX. Prior to measurement, sediment surfaces were carefully smoothed and covered with 4 μm Ultralene film to reduce surface roughness. Scans were conducted at a voltage of 10 kV, yielding count intensities for elements Al, Si, P, S, Cl, K, Ca, Ti, Cr, Mn, Fe, Rh, and Ba.

Previous studies have shown XRF core-scanning of wet sediments to be semi-quantitative due to potential limitations associated with inhomogeneity within the core, including variability in surface roughness, grain size, water content, organic material, and matrix effects (absorption/enhancement by fluorescence of other elements; e.g. Boning et al., 2007; Lowemark et al., 2011; Richter et al., 2006; Shanahan et al., 2008; Tertian and Claisse, 1982; Tjallingii et al., 2007). Therefore, the XRF element intensities

were calibrated using chemical analysis of discrete samples to obtain quantitative elemental concentrations. This analysis was conducted on select samples from core SL4 and surface samples from the Colville River catchment using a ThermoScientific Element XR, single collector ICP-MS at the Radiogenic Isotope Geosciences laboratory at Texas A&M University in College Station, TX. Total dissolution of bulk sediment samples (~0.05 g) was achieved by subsequent additions of 1 mL H₂O₂, 2 mL Aqua Regia (3HCl + HNO₃), 3 mL of HClO₄, and 8 mL HF over 190°C heat until solution was free of particulates. Following dissolution, samples were evaporated and reconstituted in a 0.02% HNO₃ solution. An internal standard (10 ppb Indium) was added to all samples to identify any mass spectrometer-induced drift effects. Calibration of the ICP-MS was achieved using external calibration solutions comprising single element standards with varying concentrations (2300–18,000 ppb for Ca, Si, and Fe; 60–1600 ppb for Mn and Ti; and 5–116 ppb for K). To test for the accuracy of our elemental analysis, the NIST standard 2702 was measured 10 times over the course of the study.

Grain size analysis

The particle size of surface samples and core SL4 (2 cm sampling interval) was analyzed on a Malvern Mastersizer 3000 laser grain-size analyzer with a measurement range of 0.02–2000 μm. Prior to measurement, 0.25–0.35 g sample splits were chemically pre-treated to remove organic material by the addition of 15 mL aliquots of 30% H₂O₂ and maintained at a temperature of 80°C until the active reaction ceased. Samples were subsequently rinsed with deionized water, centrifuged, and resuspended in a 0.05 M (NaPO₃)₆ solution to facilitate dispersion prior to addition into the fluid module. Each sample was measured six times to determine the analytical precision (0.085 μm) and 14 replicate samples per core were measured to determine the average standard deviations (0.19 μm). Errors in the D_{50} (median particle size) calculations are presented as the total combined error (0.21 μm) of analytical precision and replicate analysis. Grain size statistics were computed using the particle size analysis software GRADISTAT (Blott and Pye, 2001).

Clay mineralogy

x-Ray diffraction (XRD) analysis of clay minerals was conducted on surface samples and SL4 at a sampling interval of 4 cm. Carbonates were first removed from bulk sediment samples by the addition of 0.5 N sodium acetate–acetic acid solution at a temperature of 95°C (Strickler et al., 1989). The <2-μm sediment fractions were then separated by gravity settling in accordance with Stokes Law, and slides containing oriented grain mounts were prepared for XRD analysis. Samples were analyzed using an Empyrean x-ray diffractometer (40 kV and 40 mA) at the Louisiana State University Shared Instrument Facility. Samples were analyzed over the 4–36° 2θ interval at a step size of 0.026° 2θ. XRD scans were completed for each sample in the following four states: air-dried, ethylene glycol saturated, and heat-treated (300°C and 550°C). Peaks for the clay mineral groups – smectite, illite, kaolinite, and chlorite – were identified on the glycolated XRD run using MacDiff software, version 4.2.6 (Petschick, 2010). A quantitative representation of individual clay mineral abundance was obtained by multiplying XRD peak areas by mineral intensity factors to yield peak area percentages (PAP) following the methods of Biscaye (1965). The ethylene glycol saturation run for each sample was conducted twice to identify the instrument precision (0.527 PAP). In addition, 15 replicate samples per core were measured to obtain a replicate error of 0.898 PAP. Total standard error, a combination of the analytical and replicate errors, was calculated to be 1.04% for core SL4.

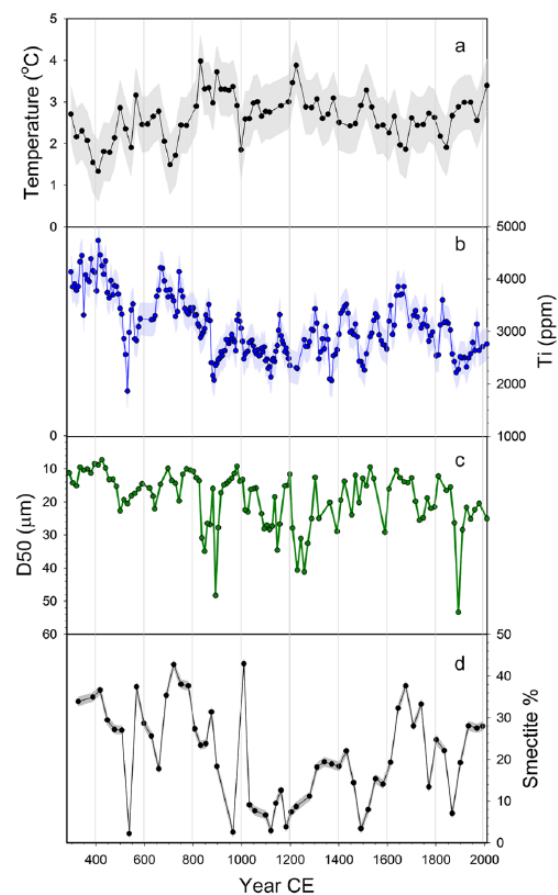


Figure 4. (a) BrGDGT-based summer temperature reconstruction for Simpson Lagoon core SL4. Gray error bands depict the 1σ bootstrap error. (b) Calculated Ti concentration for SL4. (c) Median grain size (D_{50}) for SL4; axis has been reversed to show finer sediment at the top of the plot. (d) Relative percentage of smectite for SL4.

Results

BrGDGTs

BrGDGT distributions in Simpson Lagoon core SL4 yield reconstructed temperatures ranging from 1.34°C to 3.98°C, with an overall mean of $2.66 \pm 1.06^\circ\text{C}$ (error presented as 2σ) as shown in Figure 4a. Reconstructed temperatures are generally coolest between 300 and 800 CE ($T_{\text{avg}} = 2.24 \pm 0.98^\circ\text{C}$), displaying three temperature minima centered at 410 CE ($1.34 \pm 0.72^\circ\text{C}$), 545 CE ($1.91 \pm 0.69^\circ\text{C}$), and 705 CE ($1.49 \pm 0.69^\circ\text{C}$). Temperatures then rapidly increased, reaching the warmest interval (800–1000 CE) in the approximately 1700-year record. During this interval, average temperatures were $3.31 \pm 0.65^\circ\text{C}$, with a maximum temperature of 3.98°C. The Simpson Lagoon temperature reconstruction over the past millennia reveals an overall cooling trend ($-0.9^\circ\text{C ka}^{-1}$) culminating in two temperature minima ca. 1675 CE ($1.86 \pm 0.69^\circ\text{C}$) and 1850 CE ($1.91 \pm 0.69^\circ\text{C}$). Contemporary warming over the past 150 years is characterized by a temperature increase of $\sim 1.5^\circ\text{C}$, resulting in a modern surficial temperature value of $3.40 \pm 0.62^\circ\text{C}$.

Elemental analysis

Elemental concentrations of the surface sediment samples obtained by ICP-MS measurements reveal little difference in major element (Al, Mn, Fe, Ti, Si, and K) assemblages between the terrestrial environments providing sediment to Simpson Lagoon (e.g. river, catchment tundra, and Simpson Lagoon shoreline; Table 1). However, element concentrations do vary between potential sediment

Table 1. Mean values of clay mineral abundance, median grain size, and elemental concentration with 2σ error for environments within the study area which may potentially source sediment to Simpson Lagoon.

Environment	% Smectite	% Illite	% Chlorite	% Kaolinite	D_{50} (μm)	Al (ppm)	Mn (ppm)	Fe (ppm)	Ti (ppm)	Si (ppm)	K (ppm)
River/floodplain lake ($n = 10$)	47.65 \pm 17.15	24.96 \pm 7.28	21.96 \pm 8.07	5.43 \pm 2.07	19.27 \pm 9.37	3.58 \times 10 ⁴ \pm 1.43 \times 10 ⁴	617 \pm 234	2.65 \times 10 ⁴ \pm 9.98 \times 10 ³	2720 \pm 1140	5820 \pm 3800	1.37 \times 10 ⁴ \pm 6.41 \times 10 ³
Catchment Tundra ($n = 6$)	33.16 \pm 16.42	31.57 \pm 8.01	26.79 \pm 7.08	8.47 \pm 2.22	31.97 \pm 14.97	3.66 \times 10 ⁴ \pm 5.80 \times 10 ³	679 \pm 140	2.82 \times 10 ⁴ \pm 4.73 \times 10 ³	2780 \pm 565	5300 \pm 1820	1.32 \times 10 ⁴ \pm 4.17 \times 10 ³
Shoreline Tundra ($n = 3$)	0	55.05 \pm 3.35	36.84 \pm 2.48	8.11 \pm 0.87	61.95 \pm 39.47	2.32 \times 10 ⁴ \pm 1.18 \times 10 ⁴	319 \pm 29	1.66 \times 10 ⁴ \pm 4.75 \times 10 ³	1590 \pm 702	4640 \pm 591	8.47 \times 10 ³ \pm 4.27 \times 10 ³
Beach ($n = 3$)	N/A	N/A	N/A	N/A	387.54 \pm 59.55	N/A	N/A	N/A	N/A	N/A	N/A
Colville River Braid Bar ($n = 3$)	N/A	N/A	N/A	N/A	199.54 \pm 84.26	N/A	N/A	N/A	N/A	N/A	N/A

source environments to the lagoon, with significantly lower concentrations of all measured elements in the coastal tundra bluff samples (Table 1). For the purposes of this discussion, we will focus on downcore fluctuations in the concentration of the element titanium which is commonly utilized as a proxy for terrestrial (fluvially derived) input since it is assumed to be exclusively detrital in origin and, unlike Fe and Mn, is inert to diagenetic processes in aquatic environments (Bertrand et al., 2007; Jaccard et al., 2005; Tjallingii et al., 2010; Unkel et al., 2010). Linear regression analysis reveals good correlation ($r^2 = 0.74$) between Ti concentrations (ICP-MS) and Ti intensities (XRF).

Calculated Ti concentrations for SL4 reveal multidecadal to centennial-scale fluctuations throughout the length of the core, with values ranging from 1862 to 4730 \pm 308 ppm (Figure 4b). In general, Ti concentrations are greatest during the first millennia (~350–900 CE), with an average concentration of 3553 \pm 1073 ppm. Between 900 and 1600 CE, Ti concentrations predominantly remain below the long-term mean (3070 ppm; Figure 4). Increased Ti concentrations are once again observed between ~1600 CE and 1800 CE, with calculated z -scores (a statistical value utilized to standardize the mean and variance) exceeding 1 around 1650 CE. The 20th century is characterized by lower than average Ti values (z values primarily between -0.5 and -1.5). The Ti concentration record is significantly correlated with reconstructed temperature ($r = 0.67$, $p \leq 0.01$; Pearson's correlation coefficient r is significant at p values < 0.05), with higher concentrations generally occurring during cool intervals (Figure 4a and b).

Granulometry

Grain size distributions for surface sediment samples within the Colville system are variable across environments. Sediment from the Colville River and its connected floodplain lakes, catchment tundra soils, and shoreline tundra bluffs exhibit predominantly unimodal grain size distributions that are dominated by silts and fine sands. The fluvial and tundra samples consistently contain $>60\%$ silt and clay-sized particles, with median grain size (D_{50}) of 19 \pm 9 μm and 32 \pm 15 μm , respectively. In contrast, the braid bars within the Colville River contain approximately 60–80% sand and have a median grain size of 200 \pm 84 μm . The southern shoreline bordering Simpson Lagoon consists of a narrow beach composed entirely of sand with a median grain size of 388 \pm 60 μm backed by peat-rich bluffs with a mineral component exhibiting a median grain size of 62 \pm 39 μm (Table 1).

Downcore grain size analysis of SL4 reveals a dominance of fine sediment (silts and clays, 60–99%) throughout the length of the core. However, downcore variability in the record is evident, with D_{50} values ranging between 7.33 and 53.37 \pm 0.21 μm ($\mu = 19.19$ μm , $2\sigma = 16.69$) (Figure 4c). The D_{50} record reveals coarser than average intervals occurring primarily between 800 and 1400 CE. The last ~150 years also reveals coarser sediment than the long-term average. The D_{50} record is weakly correlated with both temperature and Ti concentration ($r = 0.49$, $p \leq 0.01$; $r = 0.6$, $p \leq 0.01$, respectively), commonly exhibiting finer sediment during periods of decreased temperature and increased amounts of titanium.

Clay mineral assemblages

Clay mineral analysis reveals variability in the relative abundance of the clay mineral groups smectite, illite, chlorite, and kaolinite between environments within the study area (Table 1). Expandable minerals (i.e. smectite) comprise the largest percentage of the four clay mineral groups in the Colville River/floodplain lakes and catchment tundra sediment samples (48 \pm 17% and 33 \pm 16%, respectively). Illite and chlorite also are prominent clay minerals within the catchment (32 \pm 8% and 27 \pm 7%, respectively) and

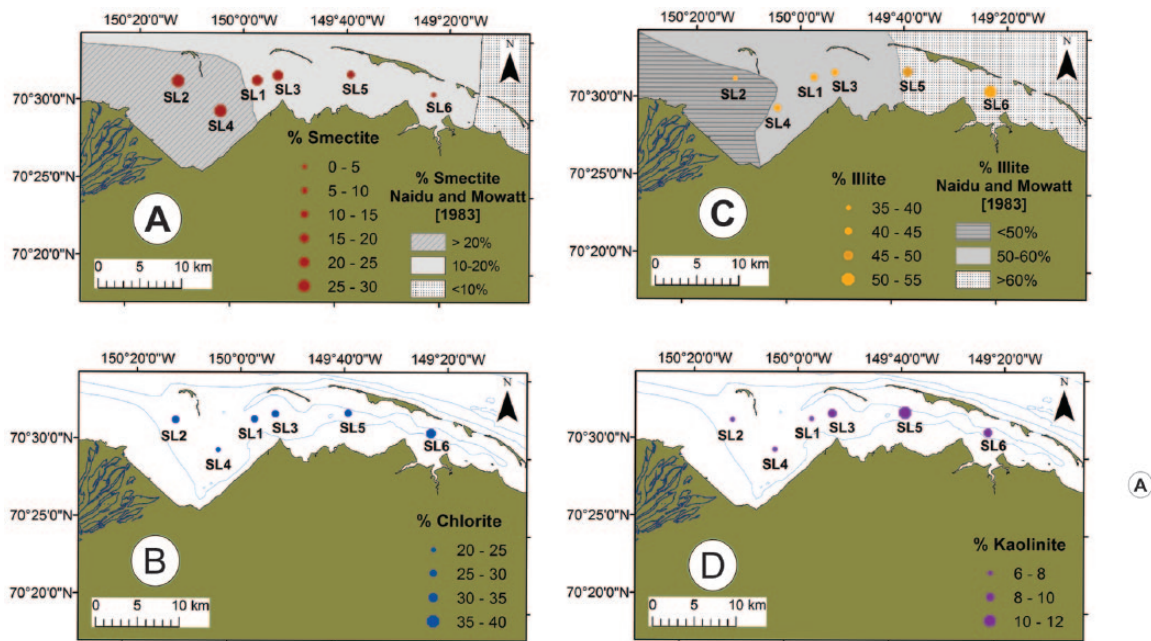


Figure 5. Relative percentages of clay mineral groups (a) smectite, (b) chlorite, (c) illite, and (d) kaolinite measured in Simpson Lagoon surface samples. Smectite abundance decreases with distance from the Colville River Delta, while the relative abundance of illite, chlorite, and kaolinite reveal an overall increase in river-distal sites. Clay mineral abundance contours from Naidu and Mowatt (1983) are plotted for smectite and illite.

river sediments ($25 \pm 7\%$, and $22 \pm 8\%$). Kaolinite comprises only 4–11% of the total clay mineral fraction. Surface samples from the shoreline bluffs bordering Simpson Lagoon, however, exhibit no measurable smectite composition. Instead, the majority of clay minerals in this coastal tundra belong to the illite group ($55.1 \pm 3.4\%$). Surficial samples from all Simpson Lagoon cores display a decreasing relative abundance of smectite and an overall increasing abundance of the other clay mineral groups with distance from the Colville River (Figure 5).

Significant temporal variability in clay mineral composition is evident in western Simpson Lagoon, with downcore measurements from SL4 exhibiting substantial fluctuations in the relative abundances of the four clay minerals (smectite range: 1–43%; illite range: 29–59%; chlorite range: 21–34%; and kaolinite range: 4–12%). Smectite abundances display the largest downcore variability as well as the greatest difference between shoreline and catchment end-member samples; therefore, further discussion of the clay mineralogy time-series will primarily focus on the smectite mineral group (shown in Figure 4d). Between ~400 and 900 CE, the abundance of smectite was greater, on average, than the long-term mean with the majority of samples containing >20% smectite (Figure 4d). This trend is reversed during the time-period extending from 900 to 1600 CE, when smectite values are predominantly $\leq 20\%$, with many samples displaying near-zero values (Figure 4d). During the past 400 years, the percentage of smectite has once again increased with values generally >20%.

Discussion

Proxy evaluation

MBT/CBT paleothermometer. The brGDGT-based MBT/CBT paleothermometer has been utilized in a variety of sediment types over the past decade, including soils (Peterse et al., 2012; Weijers et al., 2007a), lake sediments (Blaga et al., 2009; Loomis et al., 2011; Tierney et al., 2010), and coastal marine sediments (Bendle et al., 2010; Rueda et al., 2013; Weijers et al., 2007a). However, the

viability of brGDGT-based temperature reconstructions in coastal settings has recently come under scrutiny due to observations indicating significant in situ aquatic production of brGDGT in fluvial (De Jonge et al., 2014b; Zell et al., 2013a, 2013b) and marine environments (Weijers et al., 2014; Zell et al., 2014; Zhu et al., 2011). This in situ production may impart temperature signatures more representative of the aquatic environment than the expected terrestrial conditions associated with exclusive production within soils. In addition, contributions of sediment sourced to the estuarine setting via coastal erosion may complicate temperature reconstructions if these soils contain altered brGDGT distributions due to different environmental conditions.

Previous examination of potential brGDGT sources within the Colville system reveal that brGDGT distributions are consistent throughout the Colville watershed soils, shoreline sediments, Colville River sediments, and adjacent Simpson Lagoon sediments, and that in situ production within the Colville system has a limited impact on the applicability of the MBT/CBT paleothermometer in this setting (Hanna et al., 2016). In addition, reconstructed temperatures from modern sediments collected from the Colville River, catchment, shoreline tundra, and Simpson Lagoon show good agreement with instrumental summer (JJAS) air temperatures on the North Slope of Alaska, exhibiting a seasonal bias that has been observed by other researchers in high latitude settings (Pautler et al., 2014; Rueda et al., 2009, 2013; Shanahan et al., 2013). Modern reconstructed temperatures for surficial samples from SL4 are also consistent with expected summer temperatures, thus the record provided in Figure 4 likely reflects summer temperature variability over the last ~1700 years.

Simpson Lagoon, and the location where SL4 was taken, has been subjected to sediment deposition sourced from both the Colville River and direct erosion of peat-rich coastal bluffs (coastal tundra; Schreiner et al., 2013, 2014). The direct erosion of coastal peats into SL4 has the potential to dilute the temperature signal through the input of older peat layers. In all of our endmember sampling, we only found 0% smectite in the clay mineral assemblage in these coastal tundra deposits (Table 1). As described below, the amount of smectite minerals within the core

is used as a proxy for Colville-derived sediment (~30% smectite) versus peat-derived sediment (~0% smectite). Hence, to minimize the impact of this possible contamination in our interpretations, we have elected in Figure 4 and later figures (e.g. Figures 6 and 7), to remove points from all the proxy plots from depth intervals in core SL4 of <1% smectite. This was six points at Years 357, 921, 943, 987, 1076, and 1251 CE.

Records of sediment sourcing. Sediment is primarily supplied to Simpson Lagoon by coastal erosion and discharge from the Colville River (Schreiner et al., 2013, 2014). An end-member analysis of surface sediment samples in this study reveals varying elemental concentrations, clay mineralogy, and grain-size distribution between these terrestrial environments. Thus, a multi-proxy approach can be utilized to distinguish between fluvial input and coastal erosion and identify climate-driven fluctuations in the relative proportion of these two sources supplying sediment to Simpson Lagoon over the past ~1700 years.

Variations in clay mineral assemblage on the inner Alaskan Beaufort shelf are sharply defined and have previously been proposed to reflect the different clay mineral abundances associated with the major rivers of Alaska's North Slope (Naidu and Mowatt, 1974). While high abundances of illite and chlorite are fairly ubiquitous on the Beaufort shelf, relative concentrations of smectite vary significantly. Surface sediments from the Colville Delta display higher concentrations of expandable minerals ($\geq 30\%$) than any other region on the Alaskan Beaufort shelf (Naidu and Mowatt, 1983). In comparison, the coastal zone adjacent to the Kuparuk, Sagavanirktok, and Mackenzie Rivers, all located to the east of the Colville, have significantly lower relative percentages of smectite minerals ($\leq 10\%$) (Naidu and Mowatt, 1983). These previously published results, in addition to the abundance of smectite in the Colville catchment and the absence of these expandable minerals in the shoreline tundra observed in this study, suggest that this clay mineral group may be a good indicator of Colville-specific sediment sourcing (i.e. coastal erosion versus fluvial discharge) to Simpson Lagoon with smectite values exceeding ~30% indicative of predominantly Colville-derived sediment and smectite values near 0% indicative of exclusively eroded shoreline sediment.

In addition, sediments within the Colville River and catchment soils are characterized by higher concentrations of the terrestrial elements (e.g. Ti) than the coastal tundra. The lower concentration of Ti in shoreline material is potentially due to the significantly higher organic content found in the peat-rich shoreline bluffs (Schreiner et al., 2013). XRF scanners are largely insensitive to organic material in the sediment; therefore, large inputs of coastal peat may effectively dilute the lithogenic component of the sediments allowing actual concentrations of elements to be a reliable indicator of sourcing (Lowemark et al., 2011). Median particle size may also be useful in distinguishing between fluvial and coastal sediment inputs as the coastal bluffs and the bordering barrier islands generally contain coarser lithogenic grains than the tundra soils located further south in the catchment. However, the particle size of the material delivered to Simpson Lagoon via the Colville River is also dependent upon the transport energy in both the fluvial and lagoonal environments which, combined with advective processes within the lagoon (e.g. sediment winnowing, storm event resuspension/deposition), may complicate the interpretation of this record. The correlation between Ti concentrations, grain size, and clay mineralogy suggests that, if utilized together, these proxies can be used to identify changes in Colville River discharge and/or flux of sediment eroded from the coastline.

Results from surface samples from the six cores from Simpson Lagoon (Figure 1) also support our assertion that clay mineral assemblages and grain-size distributions are capable of distinguishing between fluvial and coastal sediment input. The percentage of

smectite in the clay mineral fraction of surface sediments decreases with distance from the Colville River (Figure 5), while median grain size increases in river-distal sites (Hanna et al., 2014), indicating that the relative proportion of fluvially derived sediment is greater in western Simpson Lagoon and coastal erosion likely provides a larger contribution to the total sediment deposit in eastern Simpson Lagoon. This is consistent with findings from Schreiner et al. (2013) and Zhang et al. (2015), which identified dominance of river-borne organic material in river-proximal cores and dominance of coastal-derived OM in river-distal cores.

Temperature fluctuations in Simpson Lagoon and comparison with regional records

High temporal resolution, late-Holocene temperature reconstructions from the North Slope of Alaska are sparse and have been exclusively developed from Brooks Range lake sediment archives (i.e. Charophyte calcite $\delta^{18}\text{O}$ from Tangled Up Lake (Anderson et al., 2001), varve thickness from Blue Lake (Bird et al., 2009), and chlorophyll content from Kurupa Lake (Boldt et al., 2015)). The Simpson Lagoon record presented in this study is the first temperature reconstruction, to our knowledge, developed from coastal marine sediments in the Alaskan Beaufort Sea. Comparison of the Simpson Lagoon temperature record with other North Slope and Arctic-wide reconstructions reveals variable relationships, with the Simpson Lagoon paleotemperatures most closely resembling the Arctic composite record from McKay and Kaufman (2014) over the last millennia (Figure 6a and e). This suggests that coastal marine sediment archives may provide a more regional climate reconstruction than more commonly utilized terrestrial proxies (i.e. lake sediments, tree rings). The similarity with this regional record may result from the integration of the temperature signal over the much larger Colville catchment area compared with small lake catchments. In addition, North Slope lake records may reveal a more local signal due to the complex topography and subsequent effects on atmospheric circulation patterns in the high elevations of the Brooks Range.

Climate events such as the MCA (950–1250 CE (IPCC, 2013)), LIA (1450–1850 CE (IPCC, 2013)), and 20th century warming are, however, identified in many records throughout Alaska, suggesting a regional temperature response to large-scale climatic forcings (e.g. solar irradiance, volcanic forcing, ocean-atmosphere circulation patterns) as previously postulated by Clegg et al. (2010). However, the timing and magnitude of these perturbations can vary significantly between records, potentially arising from small scale local to regional climate forcings and/or uncertainty inherent in various proxies and age models.

The low average temperatures observed in the Simpson Lagoon record before 800 CE are contemporaneous with wide-spread glacial advance in Alaska (Wiles et al., 2008). In addition, numerous lacustrine temperature reconstructions from the southern regions of Alaska exhibit cooler temperatures associated with the first millennia (Chipman et al., 2009; Clegg et al., 2010; Loso, 2009; McKay and Kaufman, 2009; Wiles et al., 2008). The more local record from Kurupa Lake (inferred from chlorophyll content) also exhibits the coolest average temperatures prior to 800 CE; however, the maximum cooling of 5.5°C in the Kurupa Lake record is significantly greater than observed in Simpson Lagoon (~2°C cooling) (Figure 6).

Temperatures warmer than the long-term (350–2010 CE) average in Simpson Lagoon persisted from ~800 to 1400 CE (Figure 4), with peak warming (~4°C) centered around 900 CE. This temperature maximum is contemporaneous (within the error of our age model, approximately ± 100 –150 years) with the early stages of the MCA and exhibits temperatures that exceed even modern temperatures. This warm perturbation is observed in other Alaskan reconstructions, although the onset and duration is variable (Bird et al., 2009; Boldt et al., 2015; Clegg et al., 2010;

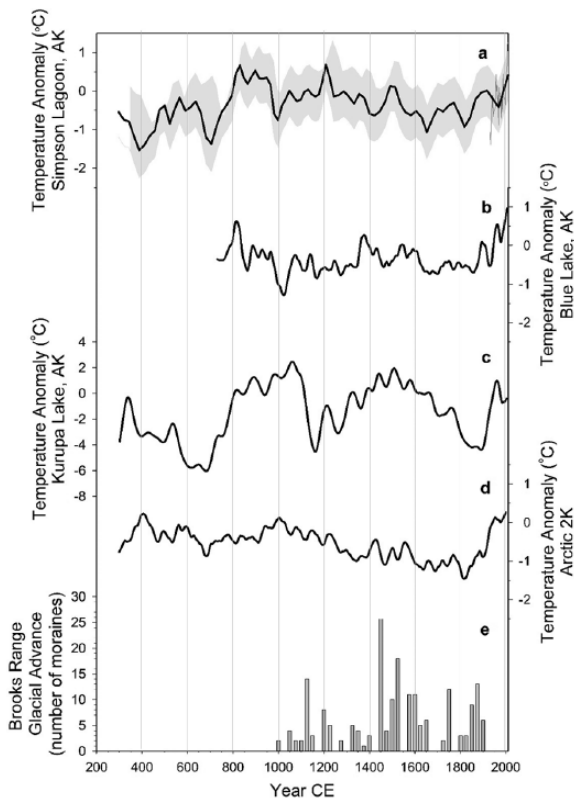


Figure 6. (a) BrGDGT-derived summer temperature anomalies from Simpson Lagoon, AK. High-resolution temperature record from core SL2 overlaid on SL4 record. (b) Varve-based summer temperature reconstruction from Blue Lake, north-central Brooks Range, AK (Bird et al., 2009). (c) Summer temperature anomaly record based on sedimentary chlorophyll content from Kurupa Lake, AK, located in the North-central Brooks Range (Boldt et al., 2015). (d) Arctic-wide composite temperature record from the PAGES Arctic 2K database (McKay and Kaufman, 2014). Temperature anomalies for all records are relative to the 1960–2000 and records have been smoothed using a 50-year running mean. (e) Frequency histogram of end moraine ages from Brooks Range glaciers based on lichenometry from Solomina and Calkin (2003).

Wiles et al., 2014). Many of these reconstructions exhibiting peak warming coeval, or just prior to, the defined MCA and reveal temperatures similar to, if not warmer than, those of the 20th century (Bird et al., 2009; Boldt et al., 2015; Wiles et al., 2014).

The shift from cooler temperatures prior to 800 CE to a warm MCA in Simpson Lagoon may result, in part, from changes in the strength/position of two prominent circulation features thought to influence temperature and precipitation in Alaska: the Aleutian Low (AL; Chipman et al., 2012; Edwards et al., 2001; Mock et al., 1998) and the Beaufort Gyre (BG; Clegg et al., 2011; Darby et al., 2012; Serreze and Barry, 2005). Late-Holocene reconstructions of the relative strength/position of the AL, based on $\delta^{18}\text{O}$ values of sedimentary calcite from Jellybean Lake in southwestern Yukon (Anderson et al., 2005), and the intensity of the BG and resultant sea-ice circulation, inferred from a record of the abundance of Kara Sea-derived Fe grains present in a Beaufort Sea core (Darby et al., 2012), illustrate a rapid intensification of both the AL and the BG occurring between ~ 700 and 900 CE. A strengthening of both circulation features would likely result in generally increased temperature/decreased precipitation over northern Alaska (Chipman et al., 2012; Clegg et al., 2011; Mock et al., 1998; Serreze and Barry, 2005).

The last millennia in the Simpson Lagoon reconstruction (with the exception of 20th century warming) are characterized by an overall cooling trend of $-0.9^\circ\text{C ka}^{-1}$. A similar trend is observed in

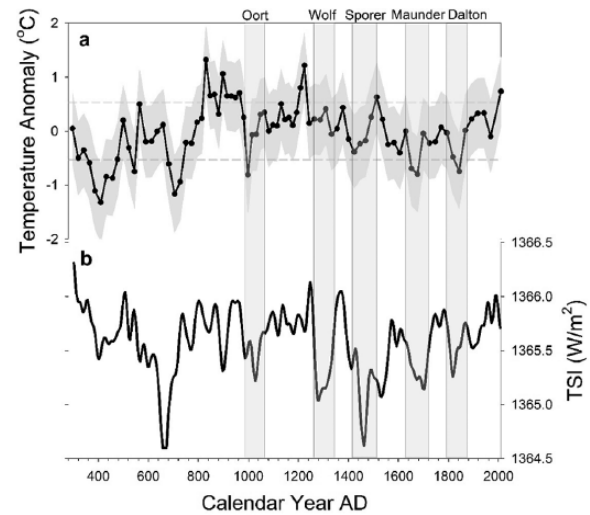


Figure 7. (a) Temperature anomaly (relative to long-term mean) for Simpson Lagoon, with 1σ deviation from the long-term mean depicted by dashed gray lines. (b) Total solar irradiance record based on Be^{10} measurements from polar ice cores (Steinhilber et al., 2012). Named solar minima (Oort, Wolf, Spörer, Maunder, and Dalton) are outlined with gray box.

the recent Arctic-wide (ARCTIC2K) composite temperature record ($-1.3^\circ\text{C ka}^{-1}$; McKay and Kaufman, 2014) and has previously been attributed to decreasing summer insolation in the northern hemisphere (Kaufman et al., 2009). The cooling in Simpson Lagoon culminates in two temperature minima ca. 1650 and 1850, which fall within the defined interval of the LIA. LIA cooling is also evident in Brooks Range records of glacial advance (Solomina and Calkin, 2003) and temperature reconstructions (Bird et al., 2009; Boldt et al., 2015), although variability in the timing of the cool phases exists (Figure 6). The LIA signal in the Simpson Lagoon record most closely resembles that of the Blue Lake varve record, with two distinct cold phases (1620–1720 CE and 1800–1850 CE). Since the LIA, temperatures in Simpson Lagoon have warmed $\sim 1.5^\circ\text{C}$, which is consistent with warming from other Brooks Range records (1.3°C , Blue Lake (Bird et al., 2009) and 1.8°C from Kurupa Lake (Boldt et al., 2015)), as well as the Arctic-wide composite record (2°C ; (McKay and Kaufman, 2014).

In Simpson Lagoon, some of the most prominent cooling events during the last millennia broadly coincide with the solar output record from Steinhilber et al. (2012) (Figure 7). The three temperature minima during this period that exceed 1σ deviation from the long-term mean (990 CE, 1660 CE, and 1850 CE) occur coeval with the Oort, Maunder, and Dalton solar irradiance minima. However, only minor cooling is observed in the Simpson Lagoon record during the Wolf and Spörer solar irradiance minima, despite the latter interval coinciding with the most extensive Brooks Range glacial advance over the past 1000 years (Solomina and Calkin, 2003; Wiles et al., 2004). Although solar irradiance is a relatively weak forcing compared with climate forcings operating at higher frequencies (e.g. atmospheric circulation, volcanic activity), a combined influence of ocean–atmosphere circulation and solar output may be the most likely mechanism for driving the observed temperature minima as suggested in previous Arctic studies (Bond et al., 2001; Wiles et al., 2004, 2008, 2014).

Climate-driven sediment sourcing to Simpson Lagoon

Simpson Lagoon records of Ti concentration, grain-size distribution, and clay mineralogy all appear to reflect relative changes in the Colville River fluvial sediment input to Simpson Lagoon over the past ~ 1700 years. Although some

variability is apparent between individual proxies, there is obvious similarity between these climate proxies throughout much of the record. In general, periods exhibiting increased proportions of fluvially derived sediment, relative to coastal sediment inputs, broadly correspond with intervals of cooler temperatures (Figure 4). Under the assumption that fluvial discharge is primarily a function of precipitation within the catchment, this relationship matches the primary synoptic climate patterns (warm/dry, cool/wet) observed over the past several decades in the Alaskan interior and North Slope (Curtis et al., 1998; Mock et al., 1998). Historical trends in precipitation and temperature during the latter half of the 20th century from the long-term climate monitoring station in Barrow, AK, also support this temperature–precipitation relationship, exhibiting a 30% decrease in total precipitation coinciding with a temperature warming of $>1^{\circ}\text{C}$ (Curtis et al., 1998). Although it is possible that climate configurations in this region may have differed in the past, this temperature–moisture relationship has also been observed in other Alaskan Holocene reconstructions during major climate events (e.g. LIA) (Anderson et al., 2001; Chipman et al., 2012; Clegg and Hu, 2010; Edwards et al., 2001; Mann et al., 2002).

Between 350 and 900 CE, Ti concentrations, median grain size, and % smectite exhibit the greatest overall deviation from the long-term mean and indicate that sediment deposition within Simpson Lagoon was likely dominated by the Colville River flux rather than coastal erosion. This is supported by the core x-radiograph (Figure 8 in Hanna et al., 2014), which exhibits millimeter- to centimeter-scale laminations consistent with fluvial sedimentation. This interval also coincides with the coolest average temperatures in the Simpson Lagoon record.

An increase in fluvial discharge during this period is supported by observations of increased moisture and/or precipitation in other North Slope records. Bird et al. (2009) found that the thickest sediment varves in a ~ 2000 -year record from Blue Lake in the north-central Brooks Range were emplaced prior to 750 CE and suggest that precipitation was the dominant control on varve thickness during this time. In addition, moisture proxies from Wolverine Lake (Mann et al., 2002) and Keche Lake (Chipman et al., 2012) also indicate intervals of higher than average precipitation during the first millennium.

The transition to warmer temperatures observed in the Simpson Lagoon record ~ 850 –900 CE broadly coincides with a transition to lower average Ti concentrations, increased intervals of coarser sediment, and substantially lower average smectite percentages (Figure 4). A variation in sediment character at ~ 900 CE is also identifiable in the CHIRP seismic record as a high-amplitude acoustic reflector and in the core x-radiograph as a thick layer of sediment characterized by low bulk density (i.e. high organic content) emplaced between 150 and 165 cm depth (Hanna et al., 2014), which may be indicative of the deposition of eroded coastal peats.

Although correlations of multi-decadal to centennial-scale fluctuations in the individual sediment sourcing proxy records are not as robust between 900 and 1600 CE as the preceding period, the overall trends in the sedimentological proxies (Ti, D_{50} , clay mineralogy) appear similar. The period between ~ 900 –1300 CE, encompassing the MCA, exhibits the lowest average concentration of titanium, greatest average D_{50} , and lowest overall abundance of smectite in the ~ 1700 -year record. Decreased discharge during this anomalously warm period is consistent with modern temperature/precipitation trends in this region. However, the modern climate conditions also suggest that significant increases in coastal erosion can occur with increased temperatures (Jones et al., 2009; Lantuit et al., 2012; Mars and Houseknecht, 2007). Warming of $\geq 1^{\circ}\text{C}$ over the latter half of the 20th century has led to a doubling of shoreline retreat

rates along the Alaskan Beaufort Sea coast (Jones et al., 2009; Mars and Houseknecht, 2007). This has primarily been attributed to an extension of the ice-free season, which increases the amount of time Arctic coasts interact with seawater and makes them more vulnerable to the frequent, highly erosive, fall frontal storms (Barnhart et al., 2014; Lantuit et al., 2012). In addition, increased temperatures can enhance degradation of the coastal permafrost, which, in turn, increases the potential for erosion. The Arctic sea ice reconstruction from Kinnard et al. (2011) suggests that sea ice is currently at its lowest extent in the past ~ 1500 years, but that periods of low sea ice cover may also have occurred prior to 1200 CE, coeval with the MCA.

In particular, the low smectite abundance (commonly $\leq 20\%$) in Simpson Lagoon between ~ 900 and 1300 CE suggests that coastal material or barrier island overwash significantly influences the total sediment deposit, as material derived from the Colville River is relatively enriched in these expandable clay minerals ($>30\%$). In addition, radiocarbon dates within this interval (~ 90 –160 cm depth) have the largest deviations from the best fit linear accumulation model and support a higher accumulation rate (Figure 2). This may be indicative of substantial pulses of coastal material, barrier overwash, or sediment mixing resulting from frontal storms, which is corroborated by a greater prevalence of coarser sediment intervals. In addition, the core x-radiograph shows evidence of storm event layers (sediment resuspension/redeposition) during this interval, characterized by basal erosional surfaces overlain by normally graded laminations.

The cool temperature intervals in Simpson Lagoon that coincide with the LIA also correspond with increases in smectite and Ti concentrations and finer sediment, all of which are indicative of increased freshwater and sediment input from the Colville River. This is broadly consistent with records of increased effective moisture in the Brooks Range during this time (Chipman et al., 2012; Clegg and Hu, 2010; Mann et al., 2002). In contrast, records from the Gulf of Alaska primarily indicate a dry LIA (Chipman et al., 2009; Daigle and Kaufman, 2009; Hu et al., 2001; Tinner et al., 2008). The difference in wet/dry conditions during the LIA between northern and southern Alaska is consistent with modern precipitation patterns and is likely related to the dominant ocean–atmosphere circulation patterns in the region (Mock et al., 1998).

Conclusion

Paleoclimate reconstructions from Simpson Lagoon, Alaska, demonstrate that Arctic coastal marine sediments provide high-resolution climate information about the late Holocene that agrees with and extends observations from other types of Arctic paleoclimate archives. The brGDGT-derived summer temperature reconstruction records previously recognized major global-scale climate events, such as the MCA, LIA, and 20th century warming, and reveals broad coherence with both regional and Arctic-wide temperature reconstructions on centennial time-scales. Comparison with potential forcing mechanisms suggests that a combination of solar irradiance and changes in the dominant atmospheric circulation patterns in the region may be driving the observed temperature variability.

In addition, pronounced fluctuations in sediment sourcing to Simpson Lagoon provide useful information for paleoclimate inferences; however, the multiple sediment sources to these environments necessitate the use of a multi-proxy approach to deconvolve potential drivers. Elemental concentrations, grain size, and clay mineralogy in Simpson Lagoon sediments reveal temporal fluctuations in Colville River water discharge as well as changes in the relative proportions of fluvial sediment input/contribution of eroded coastal sediment to Simpson Lagoon through time. Records indicate that relative increases in fluvial discharge coincided with

cooler temperatures during the first millennia and the LIA and are consistent with the primary modern temperature/precipitation patterns in northern Alaska (Mock et al., 1998), as well as Brooks Range late-Holocene effective moisture reconstructions (Chipman et al., 2012; Clegg and Hu, 2010; Mann et al., 2002), that indicate the dominance of cool/wet or warm/dry conditions. In addition, warmer intervals such as the MCA were characterized by increased input of coastally derived material and potentially decreased fluvial sediment delivery. Future efforts should be made to exploit these coastal sediment archives to increase the spatial coverage of Arctic paleoenvironmental data (both terrestrial and marine) in order to better understand past natural climate variability and the forcing mechanisms driving this change.

Acknowledgements

AJM would like to acknowledge additional support for the 2012 field program provided by the Alaskan Geological Society. The authors thank colleagues Richard Smith, Mike Rodriguez, and Captain Bill Kopplin of the R/V *Annika Marie* for all of their assistance with the 2010 field work. Assistance during the 2012 field season was provided by Peter Flaig, Dolores van der Kolk, Doug Hissom, and Stephen Hasiotis. They would also like to acknowledge Shannon Loomis for her assistance with the brGDGT statistical analysis, Franco Marcantonio and Luz Romero for assistance with elemental analysis, and Wanda LeBlanc for assistance with the XRD analysis. They also thank John Goff, Terrence Quinn, and Jud Partin for comments on early versions of this manuscript.

Funding

This research was supported by funding from the National Science Foundation (NSF EAGER grant number ARC-0935336 and NSF grant number ARC-1203851).

ORCID iD

Mead A Allison  <https://orcid.org/0000-0001-9090-1811>

References

- Anderson L, Abbott MB and Finney BP (2001) Holocene climate inferred from oxygen isotope ratios in lake sediments, Central Brooks Range, Alaska. *Quaternary Research* 55: 313–321.
- Anderson L, Abbott MB, Finney BP et al. (2005) Regional atmospheric circulation change in the North Pacific during the Holocene inferred from lacustrine carbonate oxygen isotopes, Yukon Territory, Canada. *Quaternary Research* 64: 21–35.
- Arnborg L, Walker HJ and Peippo J (1967) Suspended load in the Colville River, Alaska, 1962. *Geografiska Annaler* 49A: 131–144.
- Barnhart KR, Overeem I and Anderson RS (2014) The effect of changing sea ice on the physical vulnerability of Arctic coasts. *The Cryosphere* 8: 1777–1799.
- Batir JF, Hornbach MJ and Blackwell DD (2017) Ten years of measurements and modeling of soil temperature changes and their effects on permafrost in Northwestern Alaska. *Global and Planetary Change* 148: 55–71.
- Bendle JA, Weijers JWH, Maslin MA et al. (2010) Major changes in glacial and Holocene terrestrial temperatures and sources of organic carbon recorded in the Amazon fan by tetraether lipids. *Geochemistry, Geophysics, Geosystems* 11(12): Q12007.
- Berthier E, Schiefer E, Clarke GKC et al. (2010) Contribution of Alaskan glaciers to sea-level rise derived from satellite imagery. *Nature Geoscience* 3(2): 92–95.
- Bertrand S, Charlet F, Charlier B et al. (2007) Climate variability of southern Chile since the Last Glacial Maximum: A continuous sedimentological record from Lago Puyehue (40°S). *Journal of Paleolimnology* 39: 179–195.
- Bianchi TS and Allison MA (2009) Large-river delta-front estuaries as natural ‘recorders’ of global environmental change. *Proceedings of the National Academy of Sciences* 106(20): 8085–8092.
- Bird BW, Abbott MB, Finney BP et al. (2009) A 2000 year varve-based climate record from the central Brooks Range, Alaska. *Journal of Paleolimnology* 41: 25–41.
- Biscaye PE (1965) Mineralogy and sedimentation of recent deep-sea clay in the Atlantic Ocean and adjacent seas and oceans. *Geological Society of America Bulletin* 76: 803–832.
- Blaauw M and Christen JA (2011) Flexible Paleoclimate Age-Depth Models using an autoregressive gamma process. *Bayesian Analysis* 6(3): 457–474.
- Blaga CI, Reichert GJ, Heiri O et al. (2009) Tetraether membrane lipid distributions in water-column particulate matter and sediments: A study of 47 European lakes along a north-south transect. *Journal of Paleolimnology* 41: 523–540.
- Blott SJ and Pye K (2001) GRADISTAT: A grain size distribution and statistics package for the analysis of unconsolidated sediments. *Earth Surface Processes and Landforms* 26: 1237–1248.
- Boldt BR, Kaufman DS, McKay NP et al. (2015) Holocene summer temperature reconstruction from sedimentary chlorophyll content, with treatment of age uncertainties, Kurupa Lake, Arctic Alaska. *The Holocene* 25(4): 641–650.
- Bond G, Kromer B, Beer J et al. (2001) Persistent solar influence on North Atlantic climate during the Holocene. *Science* 294: 2130–2136.
- Boning P, Bard E and Rose J (2007) Toward, direct, micron-scale XRF elemental maps and quantitative profiles of wet marine sediments. *Geochemistry, Geophysics, Geosystems* 8(5): Q05004.
- Chipman ML, Clarke GH, Clegg BF et al. (2009) A 2000 year record of climatic change at Ongoke Lake, southwest Alaska. *Journal of Paleolimnology* 41: 57–75.
- Chipman ML, Clegg BL and Hu FS (2012) Variation in the moisture regime of northeastern interior Alaska and possible linkages to the Aleutian Low: Inferences from a late-Holocene $\delta^{18}O$ record. *Journal of Paleolimnology* 48: 69–81.
- Clegg BF and Hu FS (2010) An oxygen-isotope record of Holocene climate change in the south-central Brooks Range, Alaska. *Quaternary Science Reviews* 29(7–8): 928–939.
- Clegg BF, Clarke GH, Chipman ML et al. (2010) Six millennia of summer temperature variation based on midge analysis of lake sediments from Alaska. *Quaternary Science Reviews* 29: 3308–3316.
- Clegg BF, Kelly R, Clarke GH et al. (2011) Nonlinear response of summer temperature to Holocene insolation forcing in Alaska. *Proceedings of the National Academy of Sciences* 108(48): 19299–19304.
- Curtis J, Wendler G, Stone R et al. (1998) Precipitation decrease in the western Arctic, with special emphasis on Barrow and Barter Island, Alaska. *International Journal of Climatology* 18: 1687–1707.
- Daigle TA and Kaufman DS (2009) Holocene climate inferred from glacier extent, lake sediment and tree rings at Goat Lake, Kenai Mountains, Alaska, USA. *Journal of Quaternary Science* 24: 33–45.
- Darby DA, Ortiz JD, Grosch CE et al. (2012) 1,500-year cycle in the Arctic Oscillation identified in Holocene Arctic sea-ice drift. *Nature Geoscience* 5: 897–900.
- De Jonge C, Hopmans EC, Stadnitskaia A, et al. (2013) Identification of a novel penta- and hexamethylated branched glycerol dialkyl glycerol tetraethers in peat using HPLC-MS2, GC-MS and GC-SMB-MS. *Organic Geochemistry* 54: 78–82.
- De Jonge C, Hopmans EC, Zell CI et al. (2014a) Occurrence and abundance of 6-methyl branched glycerol dialkyl glycerol

- tetraethers in soils: Implications for palaeoclimate reconstruction. *Geochimica et Cosmochimica Acta* 141: 97–112.
- De Jonge C, Stadnitskaia A, Hopmans EC et al. (2014b) In situ produced branched glycerol dialkyl glycerol tetraethers in suspended particulate matter from the Yenisei River, Eastern Siberia. *Geochimica et Cosmochimica Acta* 125: 476–491.
- Dery SJ, Hernandez-Henriquez MA, Burford JE et al. (2009) Observational evidence of an intensifying hydrological cycle in northern Canada. *Geophysical Research Letters* 36: L13402.
- Edwards ME, Mock CJ, Finney BP et al. (2001) Potential analogues for paleoclimatic variations in eastern interior Alaska during the past 14,000 yr: Atmospheric-circulation controls of regional temperature and moisture responses. *Quaternary Science Reviews* 20: 189–202.
- Efron B (1979) Bootstrap methods: Another look at the Jackknife. *The Annals of Statistics* 7(1): 1–26.
- Eisner WR, Bockheim JG, Hinkel KM et al. (2005) Paleoenvironmental analyses of an organic deposit from an erosional landscape remnant, Arctic Coastal Plain of Alaska. *Palaeogeography, Palaeoclimatology, Palaeoecology* 217: 187–204.
- Evison LH, Calkin PE and Ellis JM (1996) Late-Holocene glaciation and twentieth-century retreat, northeastern Brooks Range, Alaska. *The Holocene* 6(1): 17–24.
- Gordeev VV (2006) Fluvial sediment flux to the Arctic Ocean. *Geomorphology* 80: 94–104.
- Hanna AJM, Allison MA, Bianchi TS et al. (2014) Late Holocene sedimentation in a high Arctic coastal setting: Simpson Lagoon and Colville Delta, Alaska. *Continental Shelf Research* 74: 11–24.
- Hanna AJM, Shanahan TS and Allison MA (2016) Distribution of branched GDGTs in surface sediments from the Colville River, Alaska: Implications for the MBT/CBT paleothermometer in Arctic marine sediments. *Journal of Geophysical Research: Biogeosciences* 121: 1762–1780.
- Hopmans EC, Weijers JWH, Schefub E et al. (2004) A novel proxy for terrestrial organic matter in sediments based on branched and isoprenoid tetraether lipids. *Earth and Planetary Science Letters* 224: 107–116.
- Hu FS, Ito E, Brown TA et al. (2001) Pronounced climatic variations in Alaska during the last two millennia. *Proceedings of the National Academy of Sciences* 98(19): 10552–10556.
- IPCC (2013) *Climate Change 2013: The Physical Science Basis. Contribution of Working Group I to the Fifth Assessment Report of the Intergovernmental Panel on Climate Change* (ed. TF Stocker, D Qin, GK Plattner et al.). Cambridge and New York: Cambridge University Press.
- Jaccard SL, Haug GH, Sigman DM et al. (2005) Glacial/interglacial changes in subarctic North Pacific stratification. *Science* 308: 1003–1006.
- Jones BM, Arp CD, Jorgenson MT et al. (2009) Increase in the rate and uniformity of coastline erosion in Arctic Alaska. *Geophysical Research Letters* 36: L03503.
- Jorgenson MT and Brown J (2005) Classification of the Alaskan Beaufort Sea Coast and estimation of carbon and sediment inputs from coastal erosion. *Geo-Marine Letters* 25: 69–80.
- Jorgenson MT, Shur YL and Pullman ER (2006) Abrupt increase in permafrost degradation in Arctic Alaska. *Geophysical Research Letters* 33: L02503.
- Kaufman DS, Schneider DP, McKay NP et al. (2009) Recent warming reverses long-term arctic cooling. *Science* 325(5945): 1236–1239.
- Kinnard C, Zdanowicz CM, Fisher DA et al. (2011) Reconstructed changes in Arctic sea ice over the past 1,450 years. *Nature* 479: 509–512.
- Lachenbruch AH and Marshall BV (1969) Heat flow in the Arctic. *Arctic* 22(3): 300–311.
- Lachenbruch AH and Marshall BV (1986) Changing climate: Geothermal evidence from permafrost in the Alaskan Arctic. *Science* 234: 689–696.
- Lantuit H, Overduin PP, Couture N et al. (2012) The Arctic coastal dynamics database: A new classification scheme and statistics on Arctic permafrost coastlines. *Estuaries and Coasts* 35: 383–400.
- Loomis SE, Russell JM and Sinninghe Damste JS (2011) Distributions of branched GDGTs in soils and lake sediments from western Uganda: Implications for a lacustrine paleothermometer. *Organic Geochemistry* 42: 739–751.
- Loomis SE, Russell JM, Ladd B et al. (2012) Calibration and application of the branched GDGT temperature proxy on East African lake sediments. *Earth and Planetary Science Letters* 357–358: 277–288.
- Loso MG (2009) Summer temperatures during the Medieval Warm Period and Little Ice Age inferred from varved proglacial lake sediments in southern Alaska. *Journal of Paleolimnology* 41: 177–128.
- Lowemark L, Chen HF, Yang TN et al. (2011) Normalizing XRF-scanner data: A cautionary note on the interpretation of high-resolution records from organic-rich lakes. *Journal of Asian Earth Science* 40: 1250–1256.
- McClelland JW, Dery SJ, Peterson BJ et al. (2006) A pan-arctic evaluation of changes in river discharge during the latter half of the 20th century. *Geophysical Research Letters* 33: L06715.
- McClelland JW, Holmes RM, Peterson BJ et al. (2004) Increasing river discharge in the Eurasian Arctic: Consideration of dams, permafrost thaw, and fires as potential agents of change. *Journal of Geophysical Research: Atmospheres* 109: D18102.
- McClelland JW, Townsend-Small A, Holmes RM et al. (2014) River export of nutrients and organic matter from the North Slope of Alaska to the Beaufort Sea. *Water Resources Research* 50: 1823–1839.
- McKay NP and Kaufman DS (2009) Holocene climate and glacier variability at Hallet and Greyling Lakes, Chugach Mountains, south-central Alaska. *Journal of Paleolimnology* 41(1): 143–159.
- McKay NP and Kaufman DS (2014) An extended Arctic proxy temperature database for the past 2,000 years. *Scientific Data* 1: 140026.
- Mahoney A, Eicken H, Gaylord AG et al. (2007) Alaska landfast sea ice: Links with bathymetry and atmospheric circulation. *Journal of Geophysical Research* 112: C02001.
- Mann DH, Heiser PA and Finney BP (2002) Holocene history of the Great Kobuk sand dunes, northwestern Alaska. *Quaternary Science Reviews* 21: 709–731.
- Mars JC and Houseknecht DW (2007) Quantitative remote sensing study indicates doubling of coastal erosion rate in past 50 yr along a segment of the Arctic coast of Alaska. *Geology* 35(7): 583–586.
- Miller GH, Alley RB, Brigham-Grette J et al. (2010) Arctic amplification: Can the past constrain the future? *Quaternary Science Reviews* 29: 1779–1790.
- Mock CJ, Bartlein PJ and Anderson PM (1998) Atmospheric circulation patterns and spatial climatic variations in Beringia. *International Journal of Climatology* 18(10): 1085–1104.
- Naidu AS and Mowatt TC (1974) Clay mineralogy and geochemistry of continental shelf sediments of the Beaufort Sea. In: Sater JC and Reed JE (eds) *The Coast and Shelf of the Beaufort Sea*. Arlington, VA: Arctic Institute of North America, pp. 493–510.
- Naidu AS and Mowatt TC (1983) Sources and dispersal patterns of clay minerals in surface sediments from the continental-shelf areas off Alaska. *Geological Society of America Bulletin* 94: 841–854.

- Osterkamp TE and Payne MW (1981) Estimates of permafrost thickness from well logs in northern Alaska. *Cold Regions Science and Technology* 5: 13–27.
- Overpeck J, Hughen K, Hardy D et al. (1997) Arctic environmental change of the last four centuries. *Science* 278: 1251–1256.
- Pautiler BG, Reichart GJ, Sanborn PT et al. (2014) Comparison of soil derived tetraether membrane lipid distributions and plant-wax δD compositions for reconstruction of Canadian Arctic temperatures. *Palaeogeography, Palaeoclimatology, Palaeoecology* 404: 78–88.
- Peterse F, van der Meer J, Schouten S et al. (2012) Revised calibration of the MBT-CBT paleotemperature proxy based on branched tetraether membrane lipids in surface soils. *Geochimica et Cosmochimica Acta* 96: 215–229.
- Peterson BJ, Holmes RM, McClelland JW et al. (2002) Increasing river discharge to the Arctic Ocean. *Science* 298: 2171–2173.
- Petschick R (2010) MacDiff 4.2.6 powder Diffraction Software. Available at: <http://www.geol-pal.uni-frankfurt.de/Staff/Hompages/Petschick/classicsoftware.html>.
- Rachold V, Grigoriev MN, Are FE et al. (2000) Coastal erosion vs riverine sediment discharge in the Arctic Shelf seas. *International Journal of Earth Sciences* 89: 450–460.
- Ray SR and Aldrich JW (1996) Flood magnitude and frequency. In: Jorgenson MT, Aldrich JW and Pullman ER (eds) *Geomorphology and Hydrology of the Colville River Delta, Alaska, 1995. Fourth Annual Report*. Fairbanks, AK: ABR Inc., pp. 35–40.
- Reimer PJ, Bard E, Bayliss A et al. (2013) IntCal13 and Marine 13 Radiocarbon Age Calibration Curves 0–50,000 years cal BP. *Radiocarbon* 55(4): 1869–1887.
- Reimnitz E, Toimil L and Barnes P (1978) Arctic continental shelf morphology related to sea-ice zonation, Beaufort Sea, Alaska. *Marine Geology* 28: 179–210.
- Richter TO, van der Gaast S, Koster B et al. (2006) The Avaatech XRF core scanner: Technical description and applications to NE Atlantic sediments. In: Rothwell RG (ed.) *New Techniques in Sediment Core Analysis*. London: Geological Society of London (Special Publications 267), pp. 39–50.
- Rueda G, Fietz S and Rosell-Mele A (2013) Coupling of air and sea surface temperatures in the eastern Fram Strait during the last 2000 years. *The Holocene* 23(5): 692–698.
- Rueda G, Rosell-Mele A, Escala M et al. (2009) Comparison of instrumental and GDGT-based estimates of sea surface and air temperatures from the Skagerrak. *Organic Geochemistry* 40: 287–291.
- Schouten S, Huguet C, Hopmans EC et al. (2007) Analytical methodology for TEX86 paleothermometry by high-performance liquid chromatography/atmospheric pressure chemical ionization-mass spectrometry. *Analytical Chemistry* 79: 2940–2944.
- Schreiner KM, Bianchi TS and Rosenheim BE (2014) Evidence for permafrost thaw and transport from an Alaskan North Slope watershed. *Geophysical Research Letters* 41: 3117–3126.
- Schreiner KM, Bianchi TS, Eglinton TI et al. (2013) Sources of terrigenous inputs to surface sediments of the Colville River Delta and Simpson's Lagoon, Beaufort Sea, Alaska. *Journal of Geophysical Research: Biogeosciences* 118: 808–824.
- Serreze MC and Barry RG (2005) *The Arctic Climate System*. Cambridge: Cambridge University Press.
- Serreze MC, Walsh JE, Chapin FS III et al. (2000) Observational evidence of recent change in the northern high-latitude environment. *Climate Change* 46: 159–207.
- Shanahan TM, Hughen KA and Van Mooy BAS (2013) Temperature sensitivity of branched and isoprenoid GDGTs in Arctic lakes. *Organic Geochemistry* 64: 119–128.
- Shanahan TM, Overpeck JT, Hubeny JB et al. (2008) Scanning micro-X-ray fluorescence elemental mapping: A new tool for the study of laminated sediment records. *Geochemistry, Geophysics, Geosystems* 9(2): Q02016.
- Sinninghe Damste JS, Hopmans EC, Pancost RD et al. (2000) Newly discovered non-isoprenoid glycerol dialkyl glycerol tetraether lipids in sediments. *Chemical Communications* 17: 1683–1684.
- Solomina O and Calkin PE (2003) Lichenometry as applied to moraines in Alaska, U.S.A., and Kamchatka, Russia. *Arctic, Antarctic, and Alpine Research* 35(2): 129–143.
- Steinhilber F, Abreu JA, Beer J et al. (2012) 9,400 years of cosmic radiation and solar activity from ice cores and tree rings. *Proceedings of the National Academy of Sciences* 109(16): 5967–5971.
- Stocker TF and Raible CC (2005) Water cycle shifts gear. *Nature* 434: 830–833.
- Stone RS and Longenecker D (2001) The advancing date of Spring snowmelt in the Alaskan Arctic. In: *Eleventh ARM Science Team Meeting Proceedings*, Atlanta, GA, 19–23 March.
- Strickler ME, Ferrell RE and Snelling RD (1989) A quantitative dissolution method for the analysis of Ca-Carbonates, mg-carbonates and Fe-carbonates in clay-rich rocks and sediments. *Journal of Sedimentary Petrology* 59(4): 624–625.
- Tertian R and Claisse F (1982) *Principles of Quantitative X-ray Fluorescence Analysis*. London: Heyden and Son Ltd.
- Tierney JE, Russell JM, Eggermont H et al. (2010) Environmental controls on branched tetraether lipid distributions in tropical East African lake sediments. *Geochimica et Cosmochimica Acta* 74: 4902–4918.
- Tinner W, Bigler C, Gedye S et al. (2008) A 700-year paleoecological record of boreal ecosystem responses to climatic variation from Alaska. *Ecology* 89(3): 729–743.
- Tjallingii R, Rohl U, Kollig M et al. (2007) Influence of the water content on X-ray fluorescence core-scanning measurements in soft marine sediments. *Geochemistry, Geophysics, Geosystems* 8(2): Q02004.
- Tjallingii R, Stattergar K, Wetzel A et al. (2010) Infilling and flooding of the Mekong River incised valley during deglacial sea-level rise. *Quaternary Science Reviews* 29: 1432–1444.
- Trefry JH, Trocine RP, Alkire MB et al. (2009) *Sources, concentrations, composition, partitioning and dispersion pathways for suspended sediments and potential metal contaminants in the Coastal Beaufort Sea*. OCS Study MMS 2009-014, Final Report. Anchorage, AK: U.S. Department of Interior, Minerals Management Service.
- Unkel I, Fernandez M, Bjorck S et al. (2010) Records of environmental changes during the Holocene from Isla de los Estados (54.4°S), southeastern Tierra del Fuego. *Global and Planetary Change* 74: 99–113.
- Walker HJ and Hudson PF (2003) Hydrologic and geomorphic processes in the Colville River Delta, Alaska. *Geomorphology* 56: 291–303.
- Weijers JWH, Schefub E, Kim JH, et al. (2014) Constraints on the sources of branched tetraether membrane lipids in distal marine sediments. *Organic Geochemistry* 72: 14–22.
- Weijers JWH, Schefub E, Schouten S et al. (2007a) Coupled thermal and hydrological evolution of tropical Africa over the last deglaciation. *Science* 315(5819): 1701–1704.
- Weijers JWH, Schouten S, van den Donker JC et al. (2007b) Environmental controls on bacterial tetraether membrane lipid distribution in soils. *Geochimica et Cosmochimica Acta* 71: 703–713.
- Wiles GC, Barclay DJ, Calkin PE et al. (2008) Century to millennial-scale temperature variations for the last two thousand years indicated from glacial geologic records of Southern Alaska. *Global and Planetary Change* 60: 115–125.

- Wiles GC, D'Arrigo RD, Barclay D et al. (2014) Surface air temperature variability reconstructed with tree rings for the Gulf of Alaska over the past 1200 years. *The Holocene* 24(2): 198–208.
- Wiles GC, D'Arrigo RD, Villalba R et al. (2004) Century-scale solar variability and Alaskan temperature change over the past millennium. *Geophysical Research Letters* 31: L15203.
- Zell C, Kim JH, Abril G et al. (2013a) Impact of seasonal hydrological variation on the distributions of tetraether lipids along the Amazon River in the central Amazon basin: Implications for the MBT/CBT paleothermometer and the BIT index. *Frontiers in Microbiology* 4: Article 228.
- Zell C, Kim JH, Hollander D, et al. (2014) Sources and distributions of branched and isoprenoid tetraether lipids on the Amazon shelf and fan: Implications for the use of GDGT-based proxies in marine sediments. *Geochimica et Cosmochimica Acta* 139: 293–312.
- Zell C, Kim JH, Moreira-Turcq P et al. (2013b) Disentangling the origins of branched tetraether lipids and crenarchaeol in the lower Amazon River: Implications for GDGT-based proxies. *Limnology and Oceanography* 58(1): 343–353.
- Zhang X, Bianchi TS and Allison MA (2015) Sources of organic matter in sediments of the Colville River delta, Alaska: A multi-proxy approach. *Organic Geochemistry* 87: 96–106.
- Zhu C, Weijers JWH, Wagner T, et al. (2011) Sources and distributions of tetraether lipids in surface sediments across a large river-dominated continental margin. *Organic Geochemistry* 42: 376–386.